Organic & Biomolecular Chemistry

Accepted Manuscript

ROYAL SOCIETY OF CHEMISTRY

www.rsc.org/obc

Submitted to Organic & Biomolecular Chemistry
Communication

Curcumin-based Molecular Probe for Near-Infrared Fluorescence Imaging of Tau Fibrils in Alzheimer's Disease[†]

Kwang-su Park,[1,‡] Yujin Seo,[1,‡] Mi Kyoung Kim,[1] Kyungdo Kim,[1] Yun Kyung Kim,[2,3] Hyunah Choo,[2,3*] and Youhoon Chong[1,*]

[1]*Department of Bioscience and Biotechnology, Bio/Molecular Informatics Center, Konkuk University, Hwayang-dong, Gwangjin-gu, Seoul 143-701, Korea;* [2]*Center for Neuro-Medicine, Korea Institute of Science and Technology, 39-1 Hawolgok-dong, Seoungbuk-gu, Seoul 136-791, Korea;* [3]*Department of Biological Chemistry, Korea University of Science and Technology, Youseong-gu, Daejeon 305-350, Korea*

[†]Electronic supplementary information (ESI) available: The synthetic procedures and characterization of the new compounds, experimental details for the preparation of aggregated tau, fluorescence-based tau-binding assay, evaluation of the fluorescent properties of the curcumin derivatives upon binding to the tau fibrils, and detection of the tau aggregates in transfected SHSY-5Y cells.

[‡]These two authors contributed equally on this work.

[*]Corresponding authors
Hyunah Choo, Ph.D., E-mail: hchoo@kist.re.kr, Tel: +82-2-958-5157
Youhoon Chong, Ph.D., E-mail: chongy@konkuk.ac.kr, Tel: +82-2-2049-6100

ABSTRACT

In recent years, there has been growing interest in the near-infrared (NIR) fluorescence imaging of tau fibrils for the early diagnosis of Alzheimer's disease (AD). In order to develop a curcumin-based NIR fluorescent probe of tau fibrils, structural modification of the curcumin scaffold was attempted by combining the following rationales: the curcumin derivative should preserve its binding affinity to the tau fibrils, and, upon binding to the tau fibrils, the probe should show favorable fluorescent properties. To meet these requirements, we designed a novel curcumin scaffold with various aromatic substituents. Among the series, the curcumin derivative **1c** with a (4-dimethylamino-2,6-dimethoxy)phenyl moiety showed a significant change in its fluorescent properties (fold increase in quantum yield, 22.9; K_d, 0.77 μM; λ_{em}, 620 nm; Φ, 0.32) after binding to tau fibrils. In addition, fluorescence imaging of tau-green fluorescent protein-transfected SHSY-5Y cells with **1c** confirmed that **1c** selectively detected tau fibrils in live cells.

Alzheimer's disease (AD), which is the most common cause of dementia, is characterized by extracellular deposits of amyloid plaques and intraneuronal deposits of neurofibrillary tangles (NFTs).[1] Although there are well-defined pathological phenotypes, there is no single test to date that can diagnose AD. Definitive confirmation of a diagnosis of AD can be obtained only with a postmortem histopathological examination of Aβ plaques and NFTs in a patient's brain. Therefore, great effort has been made to develop noninvasive methods to visualize Aβ plaques and NFTs in order to assess disease progression and monitor the effectiveness of an anti-AD agent in patients with AD.

Among the diverse optical imaging techniques, fluorescence imaging at the near-infrared (NIR) spectral region (650–900 nm) provides enormous potential as a noninvasive method for *in vivo* imaging. In the NIR region, biomolecules have low absorption and autofluorescence,[2] thus allowing an optimal penetration depth and high sensitivity. Therefore, there has been an increasing demand for new chemical entities that can be used as NIR fluorescence probes for the detection of Aβ plaques and NFTs in AD. In particular, the NIR fluorescence labeling of NFT[3] is of special interest because accumulated evidence has suggested that the severity of dementia correlates better with the load of tau fibrils than with Aβ.[4] Nevertheless, tau-targeting probes have emerged more slowly than Aβ probes, and only a handful of chemical entities that function as molecular probes for NFT[5-8] or tau aggregates[9-10] have been identified. In terms of the NIR imaging probes of tau pathology, the examples are much more limited: BODIPY-based Zn(II) complexes,[5] bis(arylvinyl)pyrimidines,[9] and CyDPA2.[10]

Curcumin (Fig. 1) is a natural yellow pigment that is derived from rhizomes of *Curcuma longa*. In addition to its well-known health-promoting benefits, curcumin has recently been recognized as an optical probe for the *in vivo* visualization of both Aβ plaques and NFTs.[11-12] However, the practical use of curcumin as an NIR contrast agent is limited because of its fluorescence emission wavelength, which is outside the NIR range (520 nm). In order to induce a redshift of the fluorescence emission, the HOMO-LUMO gap needs to be narrowed, and this is generally achieved by employing a push-pull architecture: a terminal electron-rich donor and electron-deficient acceptor groups that are bridged by a highly polarizable π-conjugated system.[13] In addition to redshifts, probes with the push-

pull architecture can be selectively turned on when they bind to the target because the nonlinear optical properties that are associated with this architecture make the fluorescence intensity susceptible to the environmental changes that are conferred by target binding.[14] Curcumin derivatives with push-pull structures have been devised and tested as NIR fluorescence probes for the *in vivo* imaging of AD pathology, and this has culminated in the recent discovery of CRANAD-2 (Fig. 1)[14] and its congeners[15] as NIR-Aβ probes. The structure of CRANAD-2 is characterized by an aromatic *N*,*N*-dimethylamino substituent and difluoroboronyl functionality that act as an electron-rich donor and an electron-deficient acceptor group, respectively. CRANAD-2 shows fluorescence emission in the NIR range (805 nm), high affinity to Aβ, and a drastic change in fluorescence properties (70-fold increase in intensity, 90 nm Stokes shift) upon binding to aggregated Aβ.[14] However, CRANAD-2 is not able to detect tau aggregates, and, to the best of our knowledge, no curcumin-based NIR probe has been reported to reveal tau fibrils.

Therefore, we were interested in developing a novel curcumin-based molecular probe that could be utilized for the NIR imaging of tau fibrils. For this purpose, structural modification of the curcumin scaffold was attempted by combining the following rationales: the curcumin derivative should preserve the binding affinity to tau fibrils, and, upon binding to the tau fibrils, the probe should show favorable fluorescence properties (emission wavelength in the NIR range and enhanced fluorescence intensity). In order to meet these requirements, a novel curcumin scaffold was designed by structural modification of CRANAD-2. (1) Through a structural comparison of CRANAD-2 and the recently reported tau-binding curcumin-sugar conjugate[16] (Fig. 1), we reasoned that the lack of tau-binding capacity by CRANAD-2 can be attributed to the difluoroboron chelate of the 1,3-diketo functionality of curcumin, and, thus, the 1,3-diketo functionality of the curcumin scaffold should be kept intact for the recognition of tau fibrils. (2) In order to induce a redshift of the fluorescence emission, a *N*,*N*-dimethylamino group, which is a well-known donor group that increases the emission wavelengths of NIR probes,[17] was positioned at the *para*-position of the aromatic ring of curcumin. (3) In addition, to enhance the tau binding as well as the fluorescence properties of the curcumin-based probes, the heretofore unexplored role of the aromatic substituent was investigated by introducing various

substituents at the *ortho* positions (R = Br, Cl, OMe, Me, H). Herein, we describe the preparation of a series of novel curcumin derivatives with a (4-dimethylamino-2,6-disubstituted)phenyl moiety (**1**, Fig. 1) and their capacity as fluorescent probes of tau fibrils.

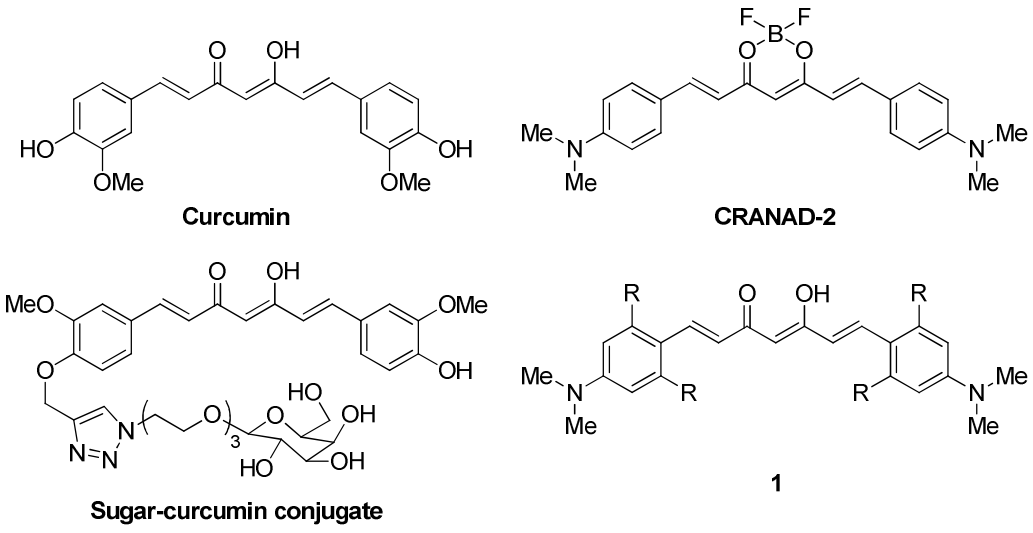

Fig. 1 Structures of the indicated compounds

Synthesis of the title compounds (**1a**–**1e**) was accomplished by the aldol condensation of acetylacetone (**6**) with appropriately substituted benzaldehydes (**5a**–**5e**)[18] (Scheme 1). Other than the commercially available **5e**, the benzaldehydes **5a**–**5d** were prepared in 1 to 4 steps starting from **2**, **3b**, **3c**, or **4d**, respectively. Thus, the reductive removal of an amino group of 2,6-dibromo-4-nitroaniline (**2**) via diazonium salt provided the aniline **3a**, which was converted into the desired benzaldehyde **5a** by *N*-methylation that was followed by a Vilsmeier-Haack reaction. Commercially available anilines (**3b** and **3c**) or *N*,*N*-dimethylaniline (**4d**) were used for preparation of the corresponding benzaldehydes (**5b**, **5c**, and **5d**) by using the same reaction conditions. Generally, the curcumin scaffold is constructed by the aldol condensation of benzaldehydes and acetylacetone in the presence of boric oxide (B_2O_3), tributyl borate [(^{n}BuO)$_3$B], and butylamine (^{n}BuNH$_2$), but this reaction results in a low chemical yield. In this study, we modified the reaction conditions by heating the reaction mixture in a sealed tube, and the synthesis of the curcumin derivatives (**1a**–**1e**) resulted in relatively

high yields (41–68%).

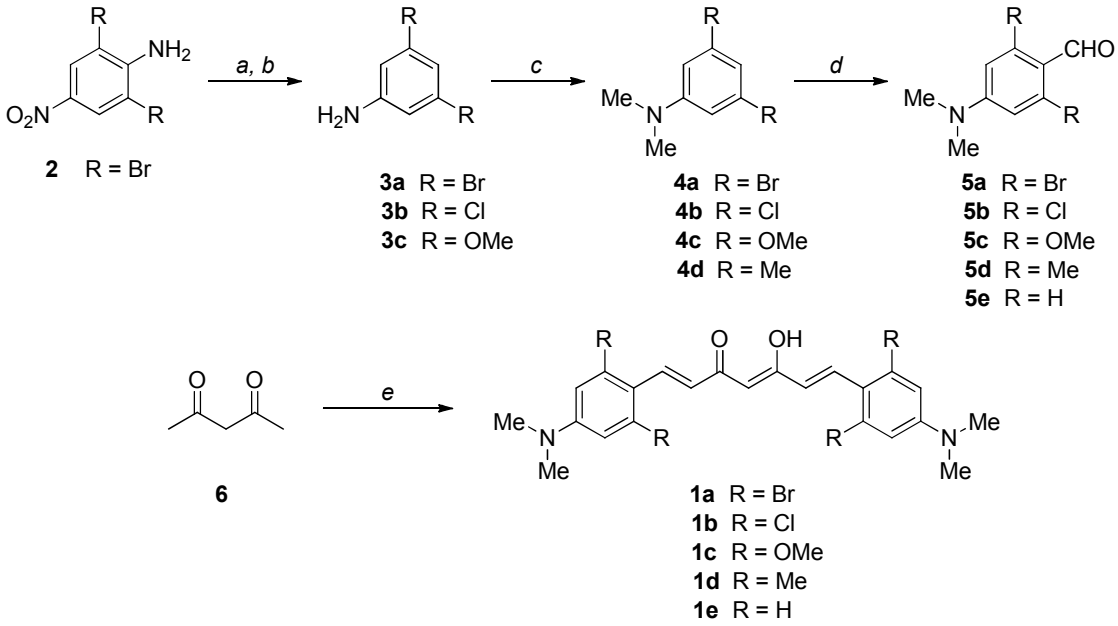

Reagents and Conditions: (a) $NaNO_2$, H_2SO_4, EtOH, 80 °C; (b) Fe, NH_4Cl, H_2O, acetone, 80 °C; (c) K_2CO_3, MeI, CH_3CN, 65 °C or CH_2O, $NaBH_3CN$, AcOH; (d) $POCl_3$, DMF, CH_2Cl_2, 0 °C; (e) **5a** - **5e**, B_2O_3, $(^nBuO)_3B$, $^nBuNH_2$, DMF

Scheme 1. Synthesis of the curcumin derivatives (**1a**–**1e**)

The prepared curcumin derivatives were evaluated for their fluorescent properties upon binding to preaggregated tau. The four-repeat tau construct K18 readily aggregated in the presence of heparin,[19] and formation of the tau fibrils was confirmed by a thioflavin-S binding assay and atomic force microscopy (Fig. S1 ~ S3 in the Supplementary Information). In order to examine the change in the fluorescent properties upon binding to tau fibrils, we compared the fluorescence spectra of the curcumin derivatives before and after mixing with tau fibrils, and the fluorescent properties are summarized in Table 1. In all of the cases, after mixing the curcumin derivatives with aggregated tau, the fluorescence quantum yields increased 1.2- to 22.9-fold. Curcumin showed a 19.1-fold increase and a Stokes shift (100 nm) in fluorescence upon binding to tau fibrils, but the maximum emission was observed only at a short wavelength (520 nm). Among the series, the curcumin derivative **1c** with *ortho*-methoxy substituents showed the most notable fluorescent properties (λ_{em}, 620 nm; Stokes shift,

120 nm; 22.9-fold quantum yield increase), which indicated that it had the desired optical properties of a useful fluorescence probe for tau fibrils. However, upon mixing with tau fibrils, other curcumin derivatives with a bromo- (**1a**), chloro- (**1b**), or methyl- (**1d**) substituent showed only slightly increased fluorescence quantum yields (1.2 ~ 1.4 fold), and these were even smaller than that of the unsubstituted analog (**1e**, 12.4 fold). On the other hand, the lipophilicity of the curcumin derivatives showed that curcumin, **1a** and **1c** possess optimum ClogP values (2.17 ~ 3.26) for penetration of blood-brain barrier (BBB) but others (**1b**, **1d** and **1e**) are too lipophilic to cross BBB (5.72 ~ 7.08).

Table 1. Changes in the fluorescence profiles of the curcumin probes (**1a**–**1e**) upon interaction with tau fibrils

Compd	ε [a] ($M^{-1}cm^{-1}$)	Unbound (free)[b]			Bound[c]			Fold increase[g]	ClogP[h]
		λ_{ex} [d] (nm)	λ_{em} [e] (nm)	QY[f] (Φ)	λ_{ex} [d] (nm)	λ_{em} [e] (nm)	QY[f] (Φ)		
Cur	54980	420	520	0.010	420	520	0.191	19.1	2.17
1a	43440	470	580	0.057	470	580	0.078	1.4	2.77
1b	52620	450	600	0.065	450	600	0.081	1.2	5.72
1c	52480	500	620	0.014	500	620	0.321	22.9	3.26
1d	32820	500	620	0.084	500	620	0.098	1.2	6.00
1e	55620	500	620	0.012	500	620	0.149	12.4	7.08

[a]Molar extinction coefficient measured in dimethylsulfoxide, [b]Fluorescence properties of the probe molecules measured in PBS without tau fibrils, [c]Fluorescence properties of the probe molecules measure in PBS with tau fibrils, [d]Maximum excitation wavelength of the probe, [e]Maximum emission wavelength of probe, [f]Quantum yield of the probe, [g]Fold increase = QY (bound) / QY (unbound, free), [h]ClogP was calculated by using ChemDraw Ultra 12.0.

Comparison of the fluorescence spectra of curcumin and its derivatives upon binding to tau fibrils (Fig. 2) provided a clue for understanding this interesting structure-property relationship. Compared

to curcumin (Fig. 2a), the curcumin derivatives with small fluorescence fold increases (**1a**, **1b** and **1d**) shared a common feature: strong native fluorescence in the absence of tau (broken lines in Fig. 2b, 2c, and 2e). In addition, fluorescence from the curcumin derivatives **1a**, **1b** and **1d** was not affected by solvents while curcumin, **1c** and **1e** showed dramatic changes in fluorescence intensities in viscous organic solvent (DMSO) (Fig. S4 in the Supplementary Information). The solvent-dependent fluorescence of curcumin, **1c** and **1e** is highly reminiscent of molecular rotors whose fluorescence emission increases when the internal free rotation is hindered due to the high viscosity of their microenvironment. In this context, the fluorescence properties of the curcumin derivatives investigated in this study can be attributed to their conformational flexibilities. Thus, sterically demanding substituents, such as Br, Cl, or Me, might constrain the internal rotation of the curcumin scaffold, and, as a result, the rigid conformations of the derivatives serve to intensify the fluorescence in the free unbound state. By the same token, the relatively low native fluorescence of the unsubstituted **1e** as well as the *ortho*-methoxy-substituted **1c** can be explained by their conformational flexibility. In particular, the internal rotation of **1c** does not seem to be hindered by the *ortho*-methoxy substituent due to the relatively small atomic size of the oxygen atom compared to the others (Br, Cl, or CH_3) as well as the bent conformation of the methoxy group, which might have resulted in the relatively low native fluorescence of **1c** (Fig. 2d).

On the other hand, upon mixing with the tau fibrils, all the curcumin derivatives showed significant fluorescence. It is noteworthy that intense fluorescence was observed from **1c** and **1e**, which might be attributed to rigidification of their conformation by binding to the tau fibrils. In order to quantitatively evaluate the binding affinity of **1c** to tau fibrils, an *in vitro* saturation-binding assay was conducted. The apparent binding constant (K_d) of **1c** was determined by plotting the fluorescence maximum at various concentrations of the probe (100, 10, 1, 0.5, 0.01, and 0.001 μM) to preaggregated tau (50 μM), and **1c** (K_d, 0.77 μM) bound to tau fibrils more favorably than thioflavin-S did (K_d, 1.90 μM, Fig. S1 in the Supplementary Information). Titration of **1c** (50 μM) with tau aggregates (Fig. S8 in the Supplementary Information) showed that fluorescence staining of tau aggregates with **1c** (lower limit of detection = 4 ng/mL) is as effective as the immunoassay (lower limit of detection = 1 ng/mL)[20] and

sensitive enough to detect the tau protein in its physiological concentration (26 ~ 66 ng/mL)[21]. The fluorescence quantum yields (Φ) of curcumin, **1c**, and **1e** were obtained in comparison to fluorescein isothiocyanate (Φ, 0.52) at pH 8 (phosphate-buffered saline) and were estimated to be 0.19, 0.32, and 0.16, respectively. The two-fold increase in the quantum yield of **1c** in comparison to curcumin or **1e** demonstrated that the methoxy substituent either strengthened the binding affinity to tau fibrils or selectively rigidified the curcumin scaffold in the tau-bound state. As was the case of curcumin[11-12], the curcumin derivative **1c** was also effective in visualization of Aβ and, upon mixing with Aβ fibrils, it showed intense fluorescence at 610 nm (Fig. S5 in the Supplementary Information).

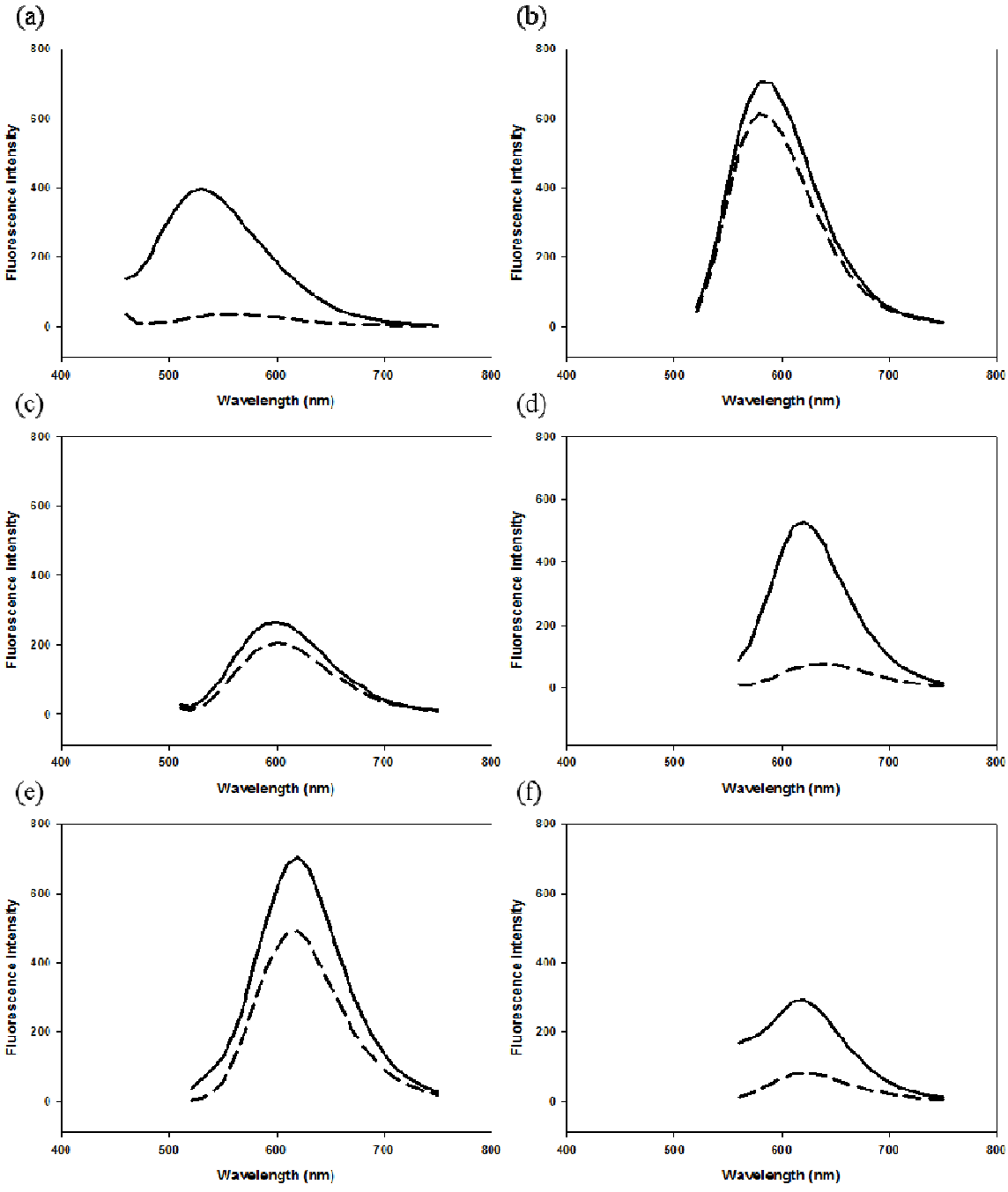

Fig. 2 Fluorescence intensities of (a) curcumin and (b–f) curcumin derivatives (**1a–1e**) (dashed line: without tau aggregate, solid line: with tau aggregate) upon interaction with aggregated tau in PBS

In order to assess whether the curcumin derivative **1c** could monitor intracellular tau aggregation, human neuroblastoma cells (SHSY-5Y) were transfected with a mammalian expression vector

expressing full-length human tau [pCMV6-htau40-green fluorescent protein (GFP)] and then treated with **1c** (Fig. 3). With confocal microscopic observation, the intracellular expression of tau-GFP was confirmed by green fluorescence (Fig. 3a). It was noteworthy that circular vacuole-like subcellular structures were observed in the transfected SHSY-5Y cells (arrows in Fig. 3a–3c), and this result was reminiscent of the findings in a previous report by Schaeffer *et al*.[22] that autophagic vacuoles are colocalized with tau inclusions. The circular structures were also intensely stained by **1c** (Fig. 3b), and the merged image (Fig. 3c) clearly showed that GFP and **1c** stained the same circular structures. In contrast, the untransfected cells without tau expression did not show fluorescence even in the presence of **1c** (Fig. S7, A and B, in the Supplementary Information). Also, the confocal microscope images of tau-GFP-transfected SHSY-5Y cells before treatment with **1c** (Figure S7, C and D, in the Supplementary Information) showed fluorescence from circular cellular compartment. In addition, blurry fluorescence presumably from tau monomers or oligomers was also observed from the cells, which is coincident with the colocalized images of GFP-tau and **1c** (Fig. 3). Taken together, the colocalization in the fluorescence microscopy images suggested that **1c** specifically detected tau aggregates in live cells.

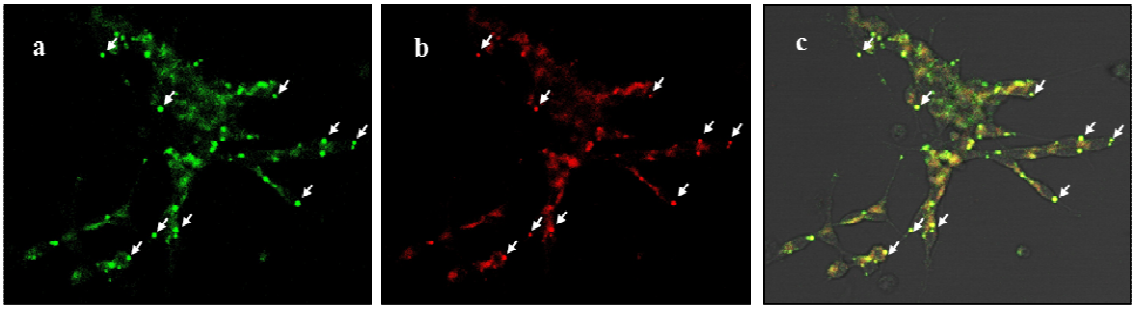

Fig. 3 Colocalization of tau aggregates and **1c** in live cell imaging. Confocal images of tau-green fluorescent protein (GFP)-transfected SH-SY5Y cells after treatment with **1c** showing dual staining for (a) GFP and (b) **1c**. (c) Merged images with the sites of colocalization shown in yellow. The tau aggregates in the vacuole-like subcellular structures are indicated by white arrows.

In summary, development of a novel curcumin-based NIR contrast agent to visualize tau fibrils was attempted. In order to optimize the fluorescent properties of the tau-binding probes, the 1,3-diketo

functionality of curcumin was kept intact while its aromatic moiety was substituted with various functionalities at the *para*- and *ortho*- positions. The newly synthesized curcumin derivatives showed fluorescence emissions at 580–620 nm but, presumably due to the rigid conformation, suffered from high native fluorescence and thereby exhibited a small increase in fluorescence intensity upon binding to tau fibrils. The only exception among the series was the curcumin derivative **1c** with a methoxy substituent, which showed a significant change in its fluorescent properties (fold increase in quantum yield, 22.9; K_d, 0.77 μM; λ_{em}, 620 nm; Φ, 0.32) after binding to tau fibrils. The small atomic size of oxygen and the bent conformation of the methoxy group might have contributed to the selective rigidification of the tau-bound conformation of **1c** while leaving the free and unbound conformation unhindered. In addition, live cell imaging of the tau-GFP-transfected SHSY-5Y cells with **1c** confirmed that **1c** specifically detected tau aggregates in live cells. Taken together, the favorable fluorescent properties upon binding to tau fibrils of **1c** suggested that it might be a promising NIR fluorescent probe for noninvasive imaging in patients with AD.

Acknowledgements

This study was supported by a grant of the Korean Health Technology R&D project, Ministry of Health & Welfare, Republic of Korea (HI14C2341) and a grant from the Priority Research Centers Program through the National Research Foundation of Korea (NRF), which is funded by the Ministry of Education, Science and Technology (2009-0093824).

Notes and references

1. D. J. Selkoe, Alzheimer's disease: genes, proteins, and therapy. *Physiol. Rev.* 2001, **81**, 741.

2. R. Weissleder, A clearer vision for in vivo imaging. *Nat. Biotechnol.* 2001, **19**, 316.

3. N.Mohorko, G. Repovš, M. Popović, G. G. Kovacs and M. Bresjanac, Curcumin labeling of neuronal fibrillar tau inclusions in human brain samples. *J. Neuropathol. Exp. Neurol.* 2010, **69**, 405.

4. C. M. Wischik, C. R. Harrington and J. M. D. Storey, Tau-aggregation inhibitor therapy for Alzheimer's disease. *Biochem. Pharmacol.* 2014, **88**, 529, and the references cited therein.

5. A. Ojida, T. Sakamoto, M. –A. Inoue, S. –H. Fujishima, G. Lippens and I. Hamachi, Fluorescence BODIPY-based Zn(II) complex as a molecular probe for selective detection of neurofibrillary tangles in the brains of Alzheimer's disease patients. *J. Am. Chem. Soc.* 2009, **131**, 6543.

6. M. Ono, S. Hayashi, K. Matsumura, H. Kimura, Y. Okamoto, M. Ihara, R. Takahashi, H. Mori and H. Saji, Rhodanine and thiohydantoin derivatives for detecting tau pathology in Alzheimer's brains. *ACS Chem. Neurosci.* 2011, **2**, 269.

7. M. T. Fodero-Tavoletti, N. Okamura, S. Furumoto, R. S. Mulligan, A. R. Connor, C. A. McLean, D. Cao, A. Rigopoulos, G. A. Cartwright, G. O'Keefe, S. Gong, P. A. Adlard, K. J. Barnham, C. C. Rowe, C. L. Masters, Y. Kudo, R. Cappai, K. Yanai and V. L. Villemagne, ^{18}F-THK523: a novel *in vivo* tau imaging ligand for Alzheimer's disease. *Brain*, 2010, **134**, 1089.

8. A. Gaghavi, S. Nasir, M. Pickhardt, R. Heyny-von Haußen, G. Mall, E. Mandelkow, E. –M. Mandelkow and B. Schmidt, N′-Benzylidene-benzohydrazides as novel and selective Tau-PHF ligands. *J. Alzheimers Dis.* 2011, **27**, 835.

9. A. Boländer, D. Kiesser, C. Voss, S. Bauer, C. Schön, S. Burgold, T. Bittner, J. Hölzer, R. Heyny-von Haußen, G. Mall, V. Goetschy, C. Czech, H. Knust, R. Berger, J. Herms, I. Hilger and B. Schmidt, Bis(arylvinyl)pyrazines, -pyrimidines, and –pyridazines as imaging agents for tau fibrils and β-amyloid plaques in Alzheimer's disease models. *J. Med. Chem.* 2012, **55**, 9170.

10. H. –Y. Kim, U. Sengupta, P. Shao, M. J. Guerrero-Munoz, R. Kayed and M. Bai, Alzheimer's disease imaging with a novel tau targeted near infrared ratiometric probe. *Am. J. Nucl. Med. Mol. Imaging*, 2013, **3**, 102.

11. M. Garcia-Alloza, L. A. Borrelli, A. Rozkalne, B. T. Hyman and B. J. Bacskai, Curcumin labels amyloid pathology *in vivo*, disrupts existing plaques, and partially restores distorted neuritis in an Alzheimer mouse model. *J. Neurochem.* 2007, **102**, 1095.

12. F. Yang, G. P. Lim, A. N. Begum, O. J. Ubeda, M. R. Simmons, S. S. Ambegaokar, P. P. Chen, R. Kayed, C. G. Glabe, S. A. Frautschy and G. M. Cole, Curcumin inhibits formation of amyloid beta

oligomers and fibrils, binds plaque, and reduces amyloid *in vivo*. *J. Biol. Chem.* 2005, **280**, 5892.

13. H. Tong, K. Lou and W. Wang, Near-infrared fluorescent probes for imaging of amyloid plaques in Alzheimer's disease. *Acta Pharm. Sin. B*. 2015, **5**, 25.
14. C. Ran, X. Xu, S. B. Raymond, B. J. Ferrara, K. Neal, B. J. Bacskai, Z. Medarova and A. Moore, Design, synthesis, and testing of difluoroboron-derivatized curcumins as near-infrared probes for in vivo detection of amyloid-β deposits. *J. Am. Chem. Soc.* 2009, **131**, 15257.
15. X. Zhang, Y. Tian, Z. Li, X. Tian, H. Sun, H. Liu, A. Moore and C. Ran, Design and synthesis of curcumin analogues for in vivo fluorescence imaging and inhibiting copper-induced cross-linking of amyloid beta species in Alzheimer's disease. *J. Am. Chem. Soc.* 2013, **135**, 16397.
16. S. Dolai, W. Shi, C. Corbo, C. Sun, S. Averick, D. Obeysekera, M. Farid, A. Alonso, P. Banerjee and K. Raja, "Clicked" sugar-curcumin conjugate: modulator of amyloid-β and tau peptide aggregation at ultralow concentrations. *ACS Chem. Neurosci.* 2011, **2**, 694.
17. (a) L. Cai, R. B. Innis and V. W. Pike, Radioligand development for PET imaging of β-amyloid (Aβ)-current status. *Curr. Med. Chem.* 2007, **14**, 19; (b) M. Cui, M. Ono, H. Kimura, H. Kawashima, B. L. Liu and H. Saji, Radioiodinated benzimidazole derivatives as single photon emission computed tomography probes for imaging of β-amyloid plaques in Alzheimer's disease. *Nucl. Med. Biol.* 2011, **38**, 313.
18. M. K. Kim, W. Jeong, J. Kang and Y. Chong, Significant enhancement in radical-scavenging activity of curcuminoids conferred by acetoxy substituent at the central methylene carbon. *Bioorg. Med. Chem.* 2011, **19**, 3793.
19. M. Pickhardt, Z. Gazova, M. von Bergen, I. Khlistunova, Y. Wang, A. Hascher, E. M. Mandelkow, J. Biernat and E. Mandelkow, Anthraquinones inhibit tau aggregation and dissolve Alzheimer's paired helical filaments in vitro and in cells. *J. Biol. Chem.* 2005, **280**, 3628.
20. C. R. Harrington, E. B. Mukaetova-Ladinska, R. Hills, P. C. Edwards, E. M. De Garcini, M. Novak and C. M. Wischik, Measurement of distinct immunochemical presentations of tau protein in Alzheimer disease. *Proc. Natl. Acad. Sci. USA*, 1991, **88**, 5842.
21. D. G. Drubin, S. C. Feinstein, E. M. Shooter and M. W. Kirschner, Nerve growth factor-induced

neurite outgrowth in PC12 cells involves the coordinate induction of microtubule assembly and assembly-promoting factors. *J. Cell Biol.* 1985, **101**, 799.

22. V. Schaeffer, I. Lavenir, S. Ozcelik, M. Tolnay, D. T. Winkler and M. Goedert, Stimulation of autophagy reduces neurodegeneration in a mouse model of human tauopathy. *Brain*, 2012, **135**, 2169.